Journal of Coordination Chemistry

ISSN: 0095-8972 (Print) 1029-0389 (Online) Journal homepage: http://www.tandfonline.com/loi/gcoo20

Coordination complexes based on V-shaped ligand and rare earth(III) ions: lanthanide contraction effect induced structural changes

Qian Cheng, Wei-Yan Huang, Qiu-Hong Huang, Yan-Ju Xiong, Jie-Fang Fang, Yun Li, Fei-Fei Zhu & Shan-Tang Yue

To cite this article: Qian Cheng, Wei-Yan Huang, Qiu-Hong Huang, Yan-Ju Xiong, Jie-Fang Fang, Yun Li, Fei-Fei Zhu & Shan-Tang Yue (2015) Coordination complexes based on V-shaped ligand and rare earth(III) ions: lanthanide contraction effect induced structural changes, Journal of Coordination Chemistry, 68:11, 1980-1996, DOI: 10.1080/00958972.2015.1038528

To link to this article: http://dx.doi.org/10.1080/00958972.2015.1038528

Journal of Coordination Chemistry, 2015
Vol. 68, No. 11, 1980–1996, http://dx.doi.org/10.1080/00958972.2015.1038528

Coordination complexes based on V-shaped ligand and rare earth(III) ions: lanthanide contraction effect induced structural changes

QIAN CHENG†, WEI-YAN HUANG†, QIU-HONG HUANG†, YAN-JU XIONG†, JIE-FANG FANG†, YUN LI†, FEI-FEI ZHU† and SHAN-TANG YUE*†‡

†School of Chemistry Environment, South China Normal University, Guangzhou, PR China
‡Guangzhou Key Laboratory of Materials for Energy Conversion and Storage, South China Normal University, Guangzhou, PR China

(*Received 16 October 2014; accepted 12 March 2015*)

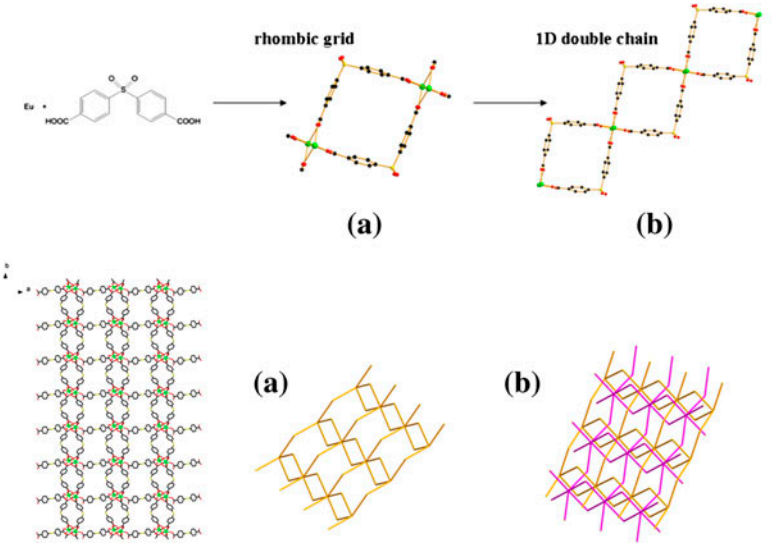

A series of metal-organic frameworks, $\{Ln_2(SDB)_3(H_2O)_5\}_n$ [Ln = Eu(**1**), Gd(**2**), Tb(**3**), Dy(**4**)], $\{[Ln_2(SDB)_3(H_2O)_4]\cdot H_2O\}_n$ [Ln = Ho(**5**), Er(**6**), Tm(**7**), Y(**8**)] and $\{[Lu_2(SDB)_3\cdot(H_2O)_3]\cdot 4H_2O\}_n$ (**9**) (H_2SDB = 4,4'-sulfonyldibenzoic acid), have been synthesized under hydrothermal conditions by using the V-shaped ligand H_2SDB. The structures of the complexes have been determined by single-crystal X-ray diffraction and further characterized using IR spectroscopy, powder X-ray diffraction, and thermogravimetric analysis. The single crystal X-ray structures show that **1–4** are isostructural featuring a 2-D weaving structure based on two chain structures containing binuclear units and organic linkers. The structures of **5–8** are analogous to those of **1–4** except that they contain coordinated solvent. Complex **9** forms a 1-D structure containing binuclear units connected by organic linkers. This series affords an opportunity to study the effect of lanthanide contraction,

*Corresponding author. Email: yuesht@scnu.edu.cn

demonstrating that the average C–S–C bond angle in coordinated H_2SDB decreases as the atomic number increases. The luminescence of **1** and **3** are also reported.

Keywords: Rare-earth complexes; V-shaped ligand; Lanthanide contraction; Luminescence properties

Introduction

There has been increasing investigation of lanthanide complexes due to their architectures and potential applications in sensing, optics, magnetism, sorption and catalysis [1]. Lanthanide metal-organic frameworks (Ln-MOFs) have received special interest as they have the characteristics of traditional lanthanide complexes, but also functional advantages of metal organic frameworks (MOFs) such as gas storage and separation [2].

MOFs and related coordination polymers are crystalline organic-inorganic hybrid materials built by linking polyatomic metal clusters by strong covalent interactions [3]. Ln-MOFs are still under development; searching in the SCI, approximately 200 papers have been published in the area. These papers find a number of useful properties of Ln-MOFs including the luminescence of Eu^{3+}-, Tb^{3+}- MOFs, the near-infrared region of Yb^{3+}-, Nd^{3+}-, Pr^{3+}- and Er^{3+}-MOFs, and the magnetic properties of Dy^{3+}- and Gd^{3+}-MOFs [4].

Ln-MOFs have been constructed using hydrothermal synthesis and a number of different aromatic multicarboxylates, such as 1,4-benzene-dicarboxylate, 4,4'-biphenyl-dicarboxylate, 1,3,5-benzene-tricarboxylate and 1,2,4,5-benzenetetracarboxylic acid [5]. These di- and polycarboxylic acids have the advantage that the carboxyl groups can chelate with metal ions [6], improving the stability of the resulting MOFs [7]. Furthermore, in combination with Ln^{3+} ions, the carboxyl groups of di- and polycarboxylic acids provide a variety of coordination modes and structures. These benefits have led to research on Ln-MOFs to focus on di- and polycarboxylic acids as ligands [7]. In contrast, studies on Ln-MOFs containing V-shaped ligands are relatively rare. V-shaped ligands are semirigid which leads to decreased stability compared to typical di- and polycarboxylic acids and subsequently, increased difficulty of synthesis. However, the structural flexibility of these ligands affords an opportunity to study the lanthanide contraction effect, as opposed to reported papers about the lanthanide contraction effects which are limited to Ln–O distances [8], the electrostatic repulsion between neighboring ligands, and the coordination number of Ln(III) [9].

To study this effect we chose 4,4′-sulfonyldibenzoic acid (H_2SDB) as our organic linker. H_2SDB is a typical example of a semirigid V-shaped dicarboxylate and has six potential donors that allow for formation of a variety of structures with different topologies [10]. Flexible O–S–O bond provides a means to study the effect of lanthanide contraction on the ligand structure in Ln-MOFs.

Several MOFs containing H_2SDB have been reported. Lin's group [7] reported alkali metal MOFs based on H_2SDB. Alkaline earth MOFs and MOFs based on transition metals like Zn^{2+}, Mn^{2+} and Co^{3+} containing H_2SDB have also been synthesized [11]. Ln-MOFs based on H_2SDB, however, are limited with the exception of three Ln-MOFs reported by Jin's group [12], one of which is a Nd^{3+}-MOF synthesized by liquid diffusion and the others are isostructural MOFs containing Yb^{3+} and Er^{3+} synthesized by the solvothermal method. Apart from this article, no Ln^{3+}-MOFs containing H_2SDB have been reported.

We report nine lanthanide MOFs, $\{Ln_2(SDB)_3(H_2O)_5\}_n$ [Ln = Eu(**1**), Gd(**2**), Tb(**3**), Dy(**4**)], $\{[Ln_2(SDB)_3(H_2O)_4]\cdot H_2O\}_n$ [Ln = Ho(**5**), Er(**6**), Tm(**7**), Y(**8**)] and $\{[Lu_2(SDB)_3\cdot$

$(H_2O)_3]\cdot 4H_2O\}_n$ (**9**), which are synthesized by using H_2SDB as a ligand under hydrothermal reaction conditions. Lanthanide contraction imposes significant effects on the Ln–O distances and C–S–C bond angles from **1** to **8**. The luminescence properties of **1** and **3** are also investigated.

Experimental

Materials and general methods

All chemicals employed were commercially available and used as received. Elemental (C, H, N) analyses were performed on a Perkin-Elmer 2400 element analyzer. The FT-IR spectra were recorded as KBr pellets from 4000 to 400 cm^{-1} on a Nicolet 5DX spectrometer. Thermogravimetric analyses (TGA) were performed on a Perkin-Elmer TGA 7 analyzer with a heating rate of 10 °C min^{-1} in air. Luminescence spectroscopy was recorded on an Edinburgh F900 FLS-900 spectrophotometer with a xenon arc lamp. In the measurement of emission and excitation spectra, the slit width was 5.0 nm. Powder X-ray diffraction (PXRD) patterns were recorded on an X-pert diffractometer or Rigaku D/M-2200T automated diffractometer using Cu K_α radiation (λ = 1.54056 Å), with a scan speed of 4°min^{-1} and a step size of 0.02° over a 2θ range of 5–50°.

Synthesis of $\{Eu_2(SDB)_3(H_2O)_5\}_n$ (1)

A mixture of $Eu(NO_3)_3\cdot 6H_2O$ (222.982 mg, 0.5 mmol), 4,4-sulfonyldibenzoic acid (H_2SDB) (153.145 mg, 0.5 mmol), and deionized water (6 mL) was placed in a 23 mL Teflon-lined stainless steel vessel. The mixture was sealed and heated at 130 °C for three days, and then cooled to room temperature at a rate of 5 °C/h. Yellow block-shaped crystals suitable for X-ray analysis were obtained in 56% yield (based on H_2SDB). Anal found/Calcd for $C_{42}H_{34}S_3Eu_2O_{23}$: C, 38.55; H, 2.65% (calculated: C, 38.59; H, 2.60%). IR (KBr, cm^{-1}): 3433(m), 2364(m), 1435(m), 1408(s), 1377(s), 1300(s), 1098(s), 1019(w), 850(w), 777(w), 736(s), 687(w), 613(m), 576(w).

Synthesis of $\{Gd_2(SDB)_3(H_2O)_5\}_n$ (2)

The process was the same as **1** except that the $Eu(NO_3)_3\cdot 6H_2O$ was replaced by Gd $(NO_3)_3\cdot 6H_2O$ (225.5 mg, 0.5 mmol). Yellow block-shaped crystals suitable for X-ray analysis were obtained in 64% yield (based on H_2SDB). Anal found/Calcd for $C_{42}H_{34}S_3Gd_2O_{23}$: C, 38.33; H, 2.61 (calculated: C, 38.28; H, 2.58%). IR (KBr, cm^{-1}): 3427(w), 2924(w), 2854(w), 2363(m), 1928(w), 1695(w), 1616(w), 1535(m), 1419(s), 1301(m), 1164(m), 1100 (m), 933(w), 860(w), 736(s), 612(m).

Synthesis of $\{Tb_2(SDB)_3(H_2O)_5\}_n$ (3)

The process was the same as **1** except that $Eu(NO_3)_3\cdot 6H_2O$ was replaced by Tb $(NO_3)_3\cdot 6H_2O$ (226.5 mg, 0.5 mmol). White block-shaped crystals suitable for X-ray analysis were obtained in 71% yield (based on H_2SDB). Anal found/Calcd for $C_{42}H_{34}S_3Tb_2O_{23}$:

C, 38.15; H, 2.55% (calculated: C, 38.19; H, 2.58%). IR (KBr, cm^{-1}): 3435(m), 2976(m), 2364(s), 1815(m), 1594(m), 1408(s), 1298(w), 1161(s), 1093(m), 861(w), 740(m), 613(m).

Synthesis of $\{Dy_2(SDB)_3(H_2O)_5\}_n$ (4)

The process was the same as **1** except that $Eu(NO_3)_3 \cdot 6H_2O$ was replaced by $Dy(NO_3)_3 \cdot 6H_2O$ (228.5 mg, 0.5 mmol). Yellow block-shaped crystals suitable for X-ray analysis were obtained in 36% yield (based on H_2SDB). Anal found/Calcd for $C_{42}H_{34}S_3Dy_2O_{23}$: C, 37.95; H, 2.53% (calculated: C, 37.98; H, 2.56%). IR (KBr, cm^{-1}): 3439(w), 2343(w), 1653(2), 1592(s), 1419(s), 1300(m), 1166(m), 1099(m), 862(w), 736(s), 613(m).

Synthesis of $\{[Ho_2(SDB)_3(H_2O)_4]\cdot H_2O\}_n$ (5)

The process was the same as **1** except that $Eu(NO_3)_3 \cdot 6H_2O$ was replaced by $Ho(NO_3)_3 \cdot 6H_2O$ (228.5 mg, 0.5 mmol). Yellow block-shaped crystals suitable for X-ray analysis were obtained in 63% yield (based on H_2SDB). Anal found/Calcd for $C_{42}H_{34}S_3Ho_2O_{23}$: C, 37.86; H, 2.58% (calculated: C, 37.84; H, 2.55%). IR (KBr, cm^{-1}): 3425(w), 2364(w), 1624(m), 1535(m), 1419(s), 1300(s), 1168(s), 1099(s), 736(s), 1014(w), 866(w), 736(s), 613(s).

Synthesis of $\{[Er_2(SDB)_3(H_2O)_4]\cdot H_2O\}_n$ (6)

The process was the same as **1** except that $Eu(NO_3)_3 \cdot 6H_2O$ was replaced by $Er(NO_3)_3 \cdot 6H_2O$ (230.5 mg, 0.5 mmol). Yellow block-shaped crystals suitable for X-ray analysis were obtained in 59% yield (based on H_2SDB). Anal found/Calcd for $C_{42}H_{34}S_3Er_2O_{23}$: C, 37.74; H, 2.56% (calculated: C, 37.71; H, 2.54%). IR (KBr, cm^{-1}): 3435(w), 2971(w), 2364(m), 1625(m), 1535(m), 1419(s), 1298(m), 1168(m), 1098(w), 1014 (w), 867(w), 740(m), 984(w).

Synthesis of $\{[Tm_2(SDB)_3(H_2O)_4]\cdot H_2O\}_n$ (7)

The process was the same as **1** except that $Eu(NO_3)_3 \cdot 6H_2O$ was replaced by Tm $(NO_3)_3 \cdot 6H_2O$ (231.5 mg, 0.5 mmol). Yellow block-shaped crystals suitable for X-ray analysis were obtained in 72% yield (based on H_2SDB). Anal found/Calcd for $C_{42}H_{34}S_3Tm_2O_{23}$: C, 37.60; H, 2.50% (calculated: C, 37.62; H, 2.54%). IR (KBr, cm^{-1}): 3435(w), 2976(m), 1625(m), 1531(s), 1415(s), 1298(s), 1167(s), 1098(s), 1051(s), 877(s), 736(s), 613(s).

Synthesis of $\{[Y_2(SDB)_3(H_2O)_4]\cdot H_2O\}_n$ (8)

The process was the same as **1** except that $Eu(NO_3)_3 \cdot 6H_2O$ was replaced by $Y(NO_3)_3 \cdot 6H_2O$ (191.5 mg, 0.5 mmol). White block-shaped crystals suitable for X-ray analysis were obtained in 66% yield (based on H_2SDB). Anal found/Calcd for $C_{42}H_{34}S_3Y_2O_{23}$: C, 42.69; H, 2.85% (calculated: C, 42.72; H, 2.88%). IR (KBr, cm^{-1}): 3430(w), 2364(w), 1624(m), 1531(m), 1419(s), 1300(m), 1168(m), 1099(m), 1014(w), 866(w), 736(m), 613(w).

Synthesis of {[Lu$_2$(SDB)$_3$·(H$_2$O)$_3$]·4H$_2$O}$_n$ (9)

The process was the same as **1** except that Eu$(NO_3)_3\cdot 6H_2O$ was replaced by Lu $(NO_3)_3\cdot 6H_2O$ (234.5 mg, 0.5 mmol). Yellow block-shaped crystals suitable for X-ray analysis were obtained in 78% yield (based on H_2SDB). Anal found/Calcd for $C_{42}H_{38}S_3Lu_2O_{25}$: C, 36.34; H, 2.76% (calculated: C, 36.31; H, 2.74%). IR (KBr, cm^{-1}): 3433(m), 2971(w), 2364(w), 1612(s), 1562(m), 1419(s), 1296(m), 1165(s), 1098(m), 1014 (m), 871(m), 782(m), 734(s), 692(m), 608(m).

Single-crystal structure determination

All these data are collected at 298 K on a Bruker Smart Apex II diffractometer with graphite-monochromated Mo K_α radiation ($\lambda = 0.71073$ Å) for **1–9**. The multiscan program SADABS is used in the absorption corrections. Structural solutions and full-matrix least-squares refinements based on F^2 were performed with SHELXS-97 and SHELXL-97 program packages, respectively [13]. The organic hydrogens were placed in geometrically idealized positions and refined using a riding model, as were the hydrogens attached to water. Details of the crystal parameters, data collections, and refinement for **1–9** are summarized in table 1.

Results and discussion

Coordination trends of Ln(III) toward H$_2$SDB

We have demonstrated that **1–9** can be synthesized using a hydrothermal reaction of Ln $(NO_3)_3\cdot 6H_2O$ with H_2SDB in H_2O. These results indicate that certain Ln^{3+} ions (specifically Eu^{3+}, Gd^{3+}, Tb^{3+}, Dy^{3+}, Ho^{3+}, Er^{3+}, Tm^{3+}, Yb^{3+}, Y^{3+} and Lu^{3+}) have affinity towards SDB. The same synthesis failed to produce frameworks when using other Ln^{3+} ions (Ce^{3+}, Pr^{3+}, Nd^{3+}, Sm^{3+} and Yb^{3+}), which is likely due to the effect of lanthanide contraction.

Structure of {Ln$_2$(SDB)$_3$(H$_2$O)$_5$}$_n$ [Ln = Eu(1), Gd(2), Tb(3), Dy(4)]

Complexes **1–4** are isostructural, so we describe **1** as an example here. Crystallographic analysis reveals that **1** crystallizes in the monoclinic P21/n space group. Single crystal X-ray diffraction studies shows that the structure of **1** possesses a 2-D weaving framework. The asymmetric unit is composed of two unique Eu(Ш) ions, three SDB ligands, and five coordinated water molecules (figure 1). Eu(1) is eight-coordinate through six oxygens on four SDB ligands (figure 1: O1, O2, O4, O6, O8, O10) and two oxygens on two water molecules (figure 1: O12a, O12b). Eu(2) is also eight-coordinate through five oxygens on SDB ligands (figure 1: O3, O5, O7, O9, O11) and three oxygens on three water molecules (figure 1: O13a, O13b, O13c). As shown in figure 2(a), four SDB ligands connect the Eu (Ш) ions forming paddle-wheel units. The SDB ligands are bent at ca. 90° forming rhombus structures linked by the paddle wheel to generate a 1-D double chain [figure 2(b)]. The chains are linked by SDB ligands bound axially to each paddle wheel forming a 2-D sheet (figure 3). Finally, the SDB ligands which link the 1-D chains are woven through the rhombus structures on a second sheet. Thus the structure is that of a 2-D woven framework which is represented in figure 4 where the Eu(III) centers are represented as a single unit.

Table 1. Crystal data and structure refinement summary for **1–9**.

Complex	**1**	**2**	**3**	**4**	**5**
Empirical formula	$C_{42}H_{34}Eu_2O_{23}$ S_3	$C_{42}H_{34}Gd_2O_{23}S_3$	$C_{42}H_{34}Tb_2O_{23}S_3$	$C_{42}H_{34}Dy_2O_{23}S_3$	$C_{42}H_{34}Ho_2O_{23}S_3$
Formula weight	1306.79	1307.29	1310.61	1327.87	1331.94
T (K)	296(2)	296(2)	296(2)	296(2)	293(2)
Crystal system	Monoclinic	Monoclinic	Monoclinic	Monoclinic	Orthorhombic
Space group	*P21/n*	*P21/n*	*P21/n*	*P21/n*	*Pbca*
a (Å)	17.868(5)	17.8594(13)	17.855(5)	17.8149(19)	12.4805(8)
b (Å)	12.848(4)	12.7942(9)	12.782(4)	12.7204(14)	22.7250(15)
c (Å)	20.456(6)	20.4258(14)	20.417(6)	20.372(2)	31.147(2)
α (°)	90	90	90	90	90
β (°)	109.646(3)	109.670(1)	109.538(3)	109.599(1)	90
γ (°)	90	90	90	90	90
V (Å^3)	4422(2)	4394.9(5)	4391(2)	4349.1(8)	8833.9(10)
Z	4	4	4	4	8
D_{Calcd} (g cm^{-3})	1.962	1.996	1.982	2.028	2.003
μ (mm^{-1})	3.043	3.226	3.429	3.646	3.790
F (0 0 0)	2576	2544	2552	2600	5210
GOF	0.704	1.001	0.812	0.842	0.849
R_1 [$I > 2\sigma(I)$][a]	0.0298	0.0353	0.0386	0.0366	0.0358
ωR_2 (all data)[b]	0.0874	0.0927	0.1347	0.1333	0.1247
Data/restraints/parameters	10,043/0/666	10,111/0/631	10,151/0/631	9906/0/631	10,314/0/634
CCDC number	1014888	1014889	1014890	1014891	1014893

Complex	**6**	**7**	**8**	**9**
Empirical formula	$C_{42}H_{34}Er_2O_{23}S_3$	$C_{42}H_{34}Tm_2O_{22}S_3$	$C_{42}H_{34}Y_2O_{23}S_3$	$C_{42}H_{38}Lu_2O_{25}S_3$
Formula weight	1337.39	1340.73	1180.71	1388.38
T (K)	296(2)	296(2)	293(2)	296(2)
Crystal system	Orthorhombic	Orthorhombic	Orthorhombic	Monoclinic
Space group	*Pbca*	*Pbca*	*Pbca*	*C2/c*
a (Å)	12.4755(19)	12.4720(18)	12.4792(19)	22.496(4)
b (Å)	22.719(4)	22.711(3)	22.727(3)	13.003(2)
c (Å)	31.116(5)	31.095(4)	31.136(5)	35.389(6)
α (°)	90	90	90	90
100.788(2)	90	90	90	93.992(2)
γ (°)	90	90	90	90
V (Å^3)	8819(2)	8808(2)	8831(2)	10,327(3)
Z	8	8	8	8
D_{Calcd} (g cm^{-3})	2.015	2.022	1.775	1.776
μ (mm^{-1})	4.014	4.237	2.849	4.006
F (0 0 0)	5232	5248	4760	5376
GOF	0.780	0.910	0.985	0.969
R_1 [$I > 2\sigma(I)$][a]	0.0316	0.0381	0.0532	0.0431
ωR_2 (all data)[b]	0.0882	0.1328	0.1075	0.1443
Data/restraints/parameters	10,301/0/630	10,520/0/606	10,357/0/631	11,912/0/649
CCDC number	1014894	1014895	1014892	1014896

[a]$R_1 = \sum||F_o| - |F_c||/\sum|F_o|$.
[b]$wR_2 = \{\sum[w(F_o^2 - F_c^2)^2]/\sum(F_o^2)^2\}^{1}$.[a]$R_1 = \sum||F_o| - |F_c||/\sum|F_o|$.
[b]$wR_2 = \{\sum[w(F_o^2 - F_c^2)^2]/\sum(F_o^2)^2\}^{1}$.

Structure of {Ln$_2$(SDB)$_3$(H$_2$O)$_4$·H$_2$O}$_n$ [Ln = Ho(5), Er(6), Tm(7), Y(8)]

The structures of **5–8** are also isostructural, so we will only describe **6** here. Crystallographic analysis of **6** reveals that it crystallizes in the orthorhombic *Pbca* space group. Single crystal X-ray diffraction shows that **6** forms a 2-D weaving framework analogous to that of **1** with

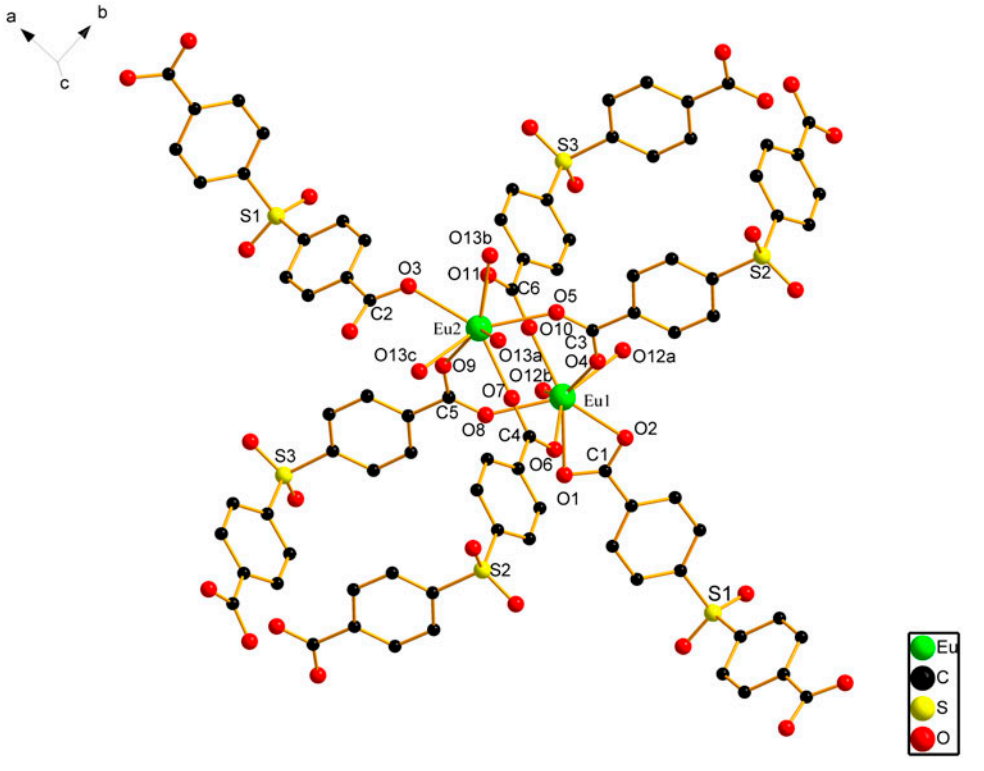

Figure 1. Coordination environment of **1**; all hydrogens were omitted for clarity [symmetry code: a = *x*, 1 + *y*, *z*; b = *x*, −1 + *y*, *z*; c = 1 + *x*, *y*, *z*].

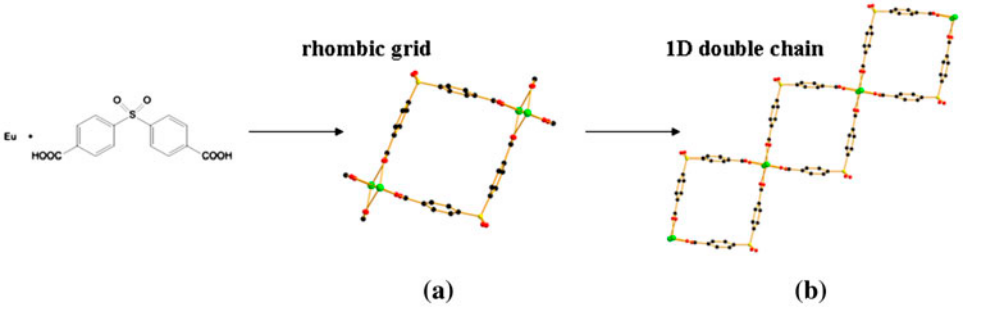

Figure 2. Schematic description of the structural component of the rhombic grid (a) and 1-D double chain (b) of **1** without hydrogens and guest solvent for clarity.

the exception that one central Er(III) ion of **6** is seven-coordinate (Er1, figure 5). In **6**, Er(1) is coordinated by only two waters (figure 5: O12a, O12b) rather than the three of **1**. The 1-D double chain, 2-D sheet, and 2-D weaving framework are shown in figures 6 and 7.

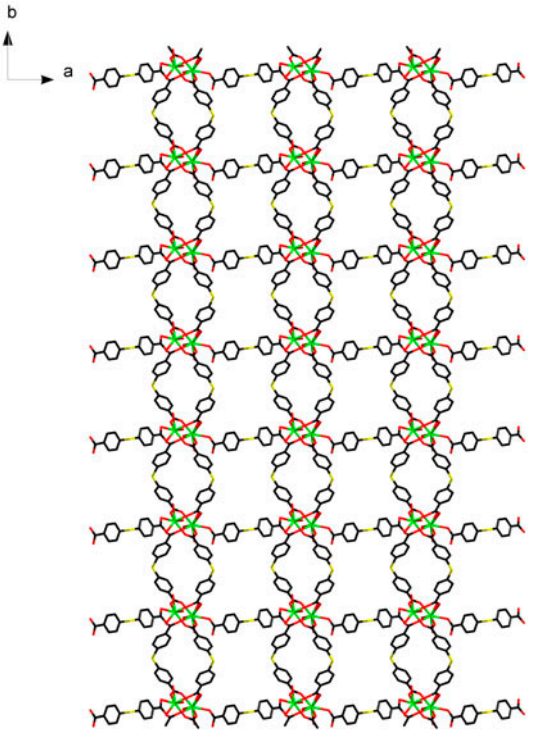

Figure 3. A polyhedral view of the 2-D layer structure constructed of 1-D chains of **1**.

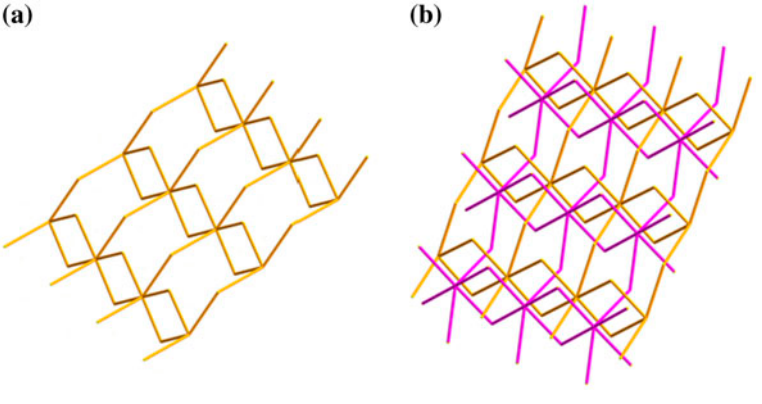

Figure 4. (a) Topological structure of the 2-D layer in **1**; (b) topological structure of the interspersed supermolecular structure of **1**.

Structure of {Lu$_2$(SDB)$_3$(H$_2$O)$_3$·4H$_2$O}$_n$ (9)

Single crystal X-ray diffraction shows that **9** crystallizes in the monoclinic space group *C2/c*. In contrast to the first two structures, **9** forms a 1-D chain structure. The asymmetric unit consists of two Lu(III) ions, three SDB ligands and three coordinated waters. Lu(1) is

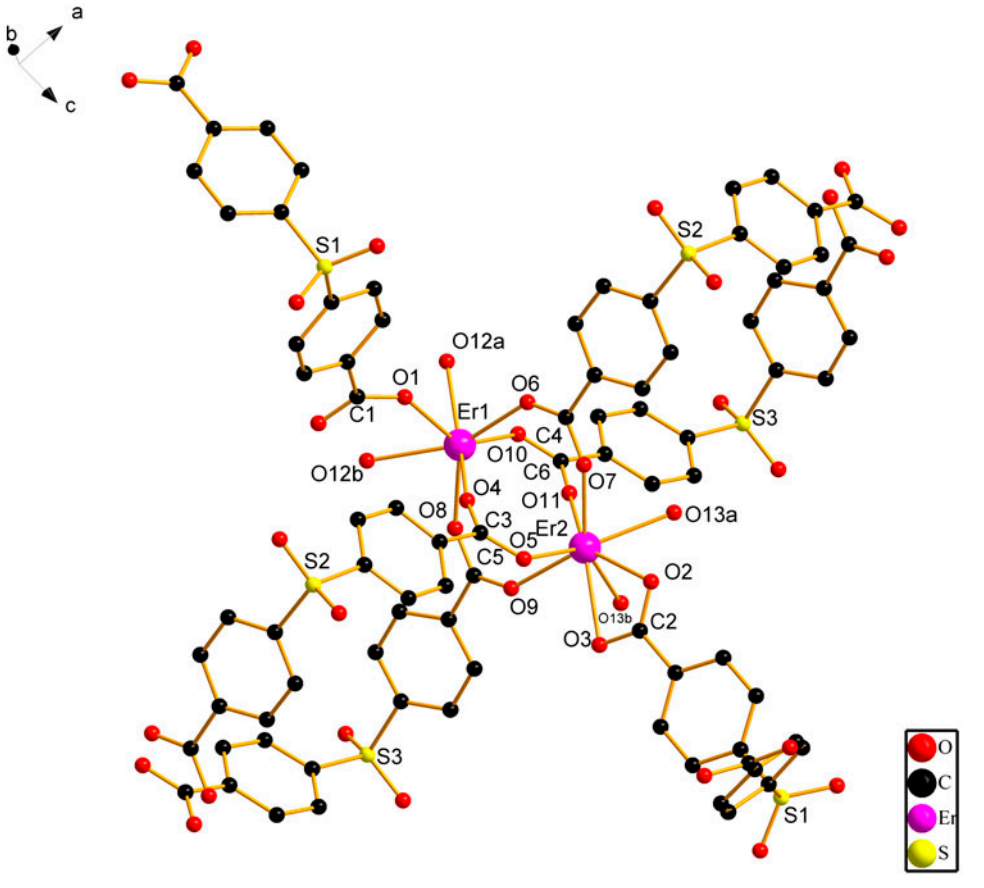

Figure 5. Coordination environment of **6**; all hydrogens were omitted for clarity [symmetry code: a = −1 + *x*, *y*, *z*; b = *x*, 0.5 − *y*, −0.5 + *z*].

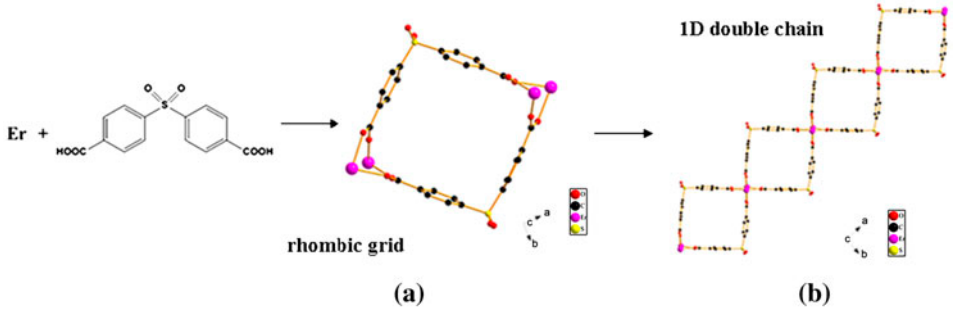

Figure 6. Schematic description of the structural component of the rhombic grid (a) and 1-D double chain (b) of **6** without hydrogens and guest solvent for clarity.

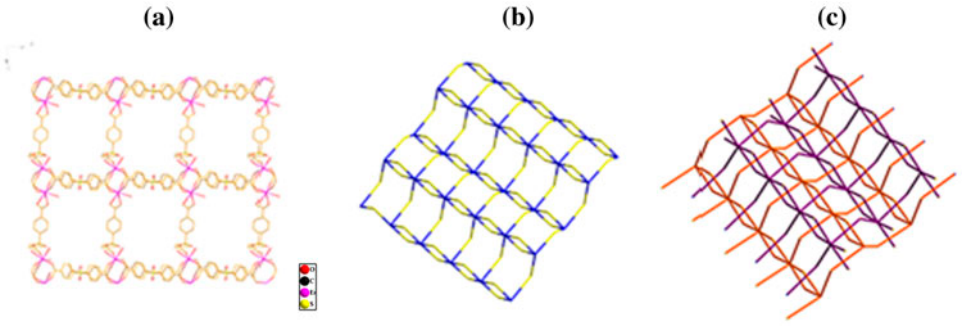

Figure 7. (a) A polyhedral view of the 2-D layer structure constructed of 1-D chains for **6**; (b) the topological structure of the 2-D layer for **6**; (c) the topological structure constructed by two layers interspersing each other for **6**.

eight-coordinate through six oxygens from the four coordinated SDB linkers (figure 8: O1, O2, O3, O4, O5, O6) and two oxygens from water molecules (figure 8: O13, O14). The Lu(2) site is seven-coordinate and is bridged to the Lu(1) site by the carboxyl groups on two SDB ligands (figure 8: S2), coordinated to four oxygens from four more SDB ligands which bridge adjacent Lu(2) sites (figure 8: O8, O10, O11a, O9a) and also by a single water (figure 8: O15). Two SDB (S3, S4) ligands (figure 8) bridge adjacent asymmetric units which ultimately results in formation of an extended 1-D chain [figure 9(a) and (b)].

Jin's group [12] reported isostructural MOFs also containing the paddle-wheel units. They are synthesized with Yb^{3+} and Er^{3+}, respectively. Different from **1** in that four SDB ligands connect Eu(1) and Eu(2) ions forming paddle-wheel units, the same two Yb^{3+} or Er^{3+} ions are included in the paddle-wheel units, then generate two 1-D double chains and one SDB links them to form a 3-D structure. Kitagawa's group [11] has reported the paddlewheel structure using Zn^{2+} ions and SDB ligands; thus SDB is apt to generate the paddlewheel units as ligands.

Thermal analysis

In order to characterize the series of Ln-MOFs more fully in terms of thermal stability, TGA experiments were investigated on samples from 30 to 800 °C with a heating rate of 10 °C min^{-1} in dry air (figures S1–9 [see online supplemental material at http://dx.doi.org/10.1080/00958972.2015.1038528]). For **1**, weight loss is observed until it reaches 100–150 °C, from release of coordinated water (observed, 7.96%; calculated, 7.89%), and then decomposition of the ligands at 430 °C. The TG lines of **3** overlap almost completely with **1**. Compound **2** is similar to **4**, the initial weight loss is observed at 90–200 °C, which is attributed to release of coordinated solvent (**2**: observed, 7.97%; calculated, 7.91%, **4**: observed, 7.97%; calculated, 7.95%). Then, the frameworks look stable to 450 °C. Compounds **5** and **7** also have two steps of weight losses, the first at 105 °C, which is attributed to release of coordinated water and crystal-lattice water (**5**: observed, 6.71%; calculated, 6.75%, **7**: observed, 6.77%; calculated, 6.74%), and then the decomposition of the ligands at 440 °C. For **6**, the first loss is observed at 102 °C, attributed to release of coordinated water (observed, 4.85%; calculated, 4.88%), then release of free water (observed, 2.05%; calculated, 2.01%), the second weight loss is under 260 °C, the decomposition of the framework

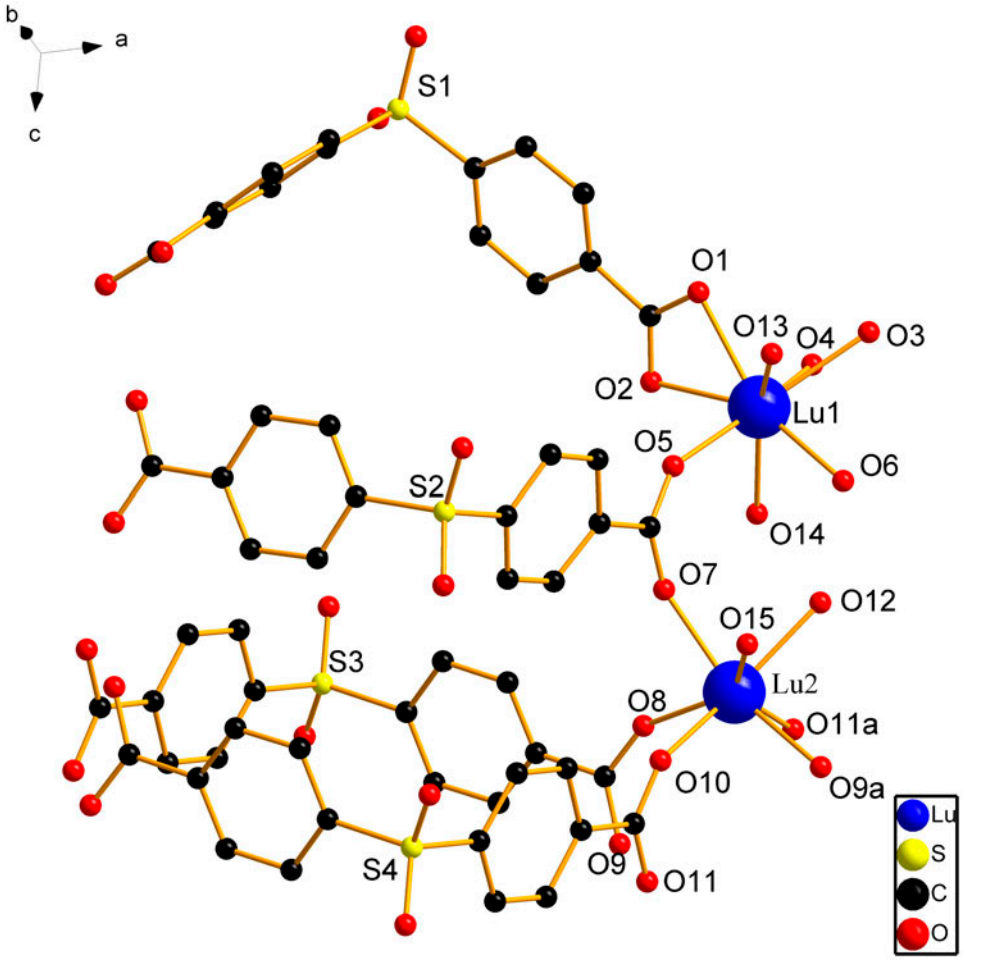

Figure 8. Coordination environment of **9**; all hydrogens were omitted for clarity [symmetry code: a = −*x*, 2 − *y*, −*z*; b = 0.5 − *x*, 1.5 − *y*, −*z*; c = 0.5 + *x*, −0.5 + *y*, *z*].

occurs at 475 °C. The TGA curve of **8** shows a weight loss process under 150 °C, corresponding to loss of water (observed, 7.68%; calculated, 7.63%). The further weight loss at 480 °C represents the decomposition of the ligands. For **9**, weight loss at 100 °C is consistent with loss of four crystal-lattice water (observed, 5.17%; calculated, 5.19%), at 195 °C, the weight loss is consistent with the loss of three coordinated waters (observed, 3.85%; calculated, 3.89%), and then a plateau region follows until 460 °C. Further weight losses represent decomposition of the ligands.

X-ray powder diffraction (PXRD)

PXRD experiments were carried out on **1–9** to determine whether the crystal structures are truly representative of the bulk materials (figures S10–18, Supporting Information). The experimental patterns and patterns simulated from the crystal structures are in agreement, suggesting that this is indeed the case.

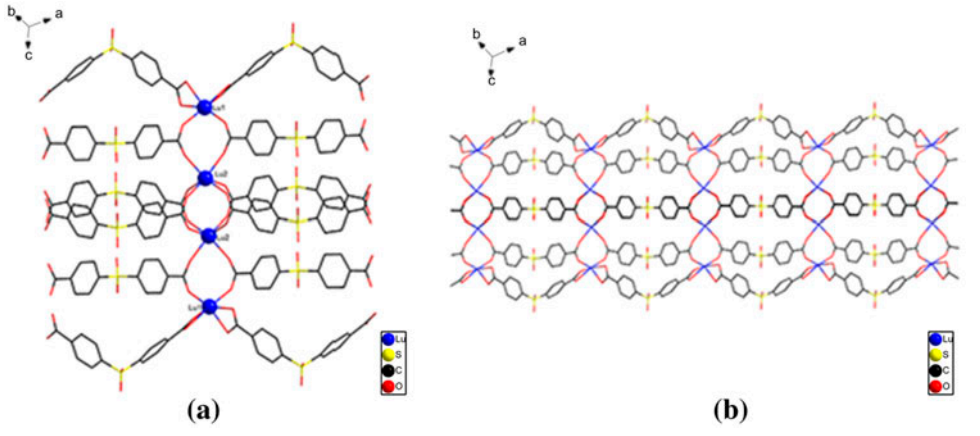

Figure 9. (a) Elementary unit of 1-D chain for **9**; (b) 1-D chain for **9**; all hydrogens were omitted for clarity.

Luminescent properties

Luminescent properties of compounds containing d^{10} metal centers are of intense interest due to their potential applications in chemical sensors, photochemistry, electroluminescent displays, etc. [14]. As lanthanide complexes often have excellent luminescent properties, the solid-state luminescence of 40 mg of **1** and **3** was investigated at room temperature. Upon excitation at 394 nm, **1** displays strong red luminescence with four characteristic emission bands for f-f transitions of Eu(III) ions [figure 10(a)]. The emission bands at 591 nm ($^5D_0 \rightarrow {}^7F_1$), 617 nm ($^5D_0 \rightarrow {}^7F_2$), 654 nm ($^5D_0 \rightarrow {}^7F_3$) and 704 nm ($^5D_0 \rightarrow {}^7F_4$) are attributed to $^5D_0 \rightarrow {}^7F_J$ ($J = 1 \rightarrow 4$) transitions [15]. The $^5D_0 \rightarrow {}^7F_1$ transition at 591 nm is a magnetic dipole allowed transition. The emission peak at 617 nm can be attributed to the hypersensitive electric dipole transition $^5D_0 \rightarrow {}^7F_2$, as it is the strongest emission and its intensity increases as the site symmetry decreases, resulting in a brilliant-red emission [16].

When excited at 370 nm, the emission spectrum of **3** exhibits green luminescence with emission bands characteristic of Tb(III) ions, centered at 490 nm ($^5D_4 \rightarrow {}^7F_6$), 545 nm ($^5D_4 \rightarrow {}^7F_5$), 585 nm ($^5D_4 \rightarrow {}^7F_4$) and 622 nm ($^5D_4 \rightarrow {}^7F_3$) [figure 10(b)]. These transitions result from deactivation of the $^5D_4$ excited state to the corresponding ground state, ^7F_J ($J = 2 \rightarrow 6$) of Tb(III) ions. Comparing the luminescence spectra of **1** and **3** shows **3** is more emissive than **1**, indicating that the Tb(III) interacts more strongly with the organic ligand than Eu(III) [17].

Analysis of lanthanide contraction effect

Although we have generated three distinct structures of Ln-MOFs, we find that the LnMOFs containing Eu(III) through Tm(III) are nearly isostructural. Therefore this series provides an opportunity for direct experimental evaluation of lanthanide contraction [8].

It is apparent that the lanthanide contraction effect results in decreasing of the Ln(III)–$O_{carbonyl}$ bond lengths. As shown in table 2, the average Ln(III)–$O_{carbonyl}$ bond lengths of **1–7** are 2.4000, 2.3865, 2.3737, 2.3546, 2.3284, 2.3202 and 2.3094,

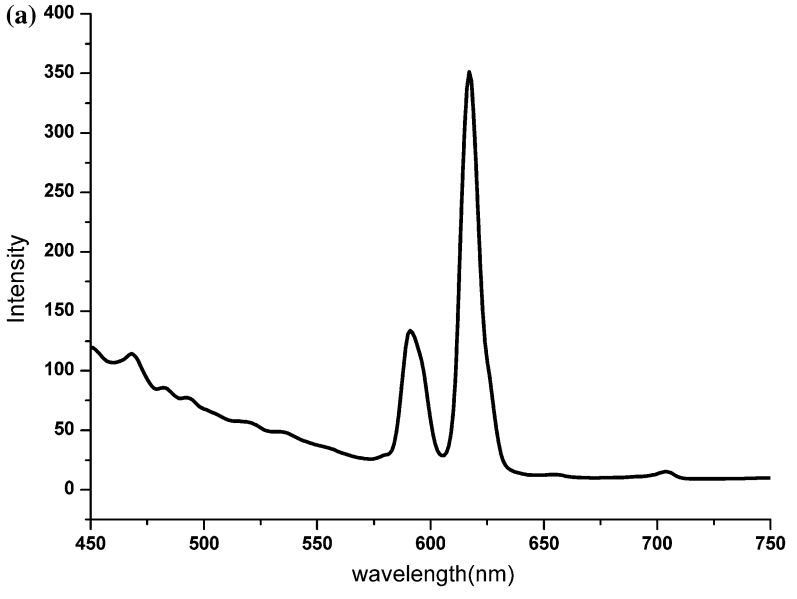

Figure 10a. Solid-state emission spectra at room temperature for **1**.

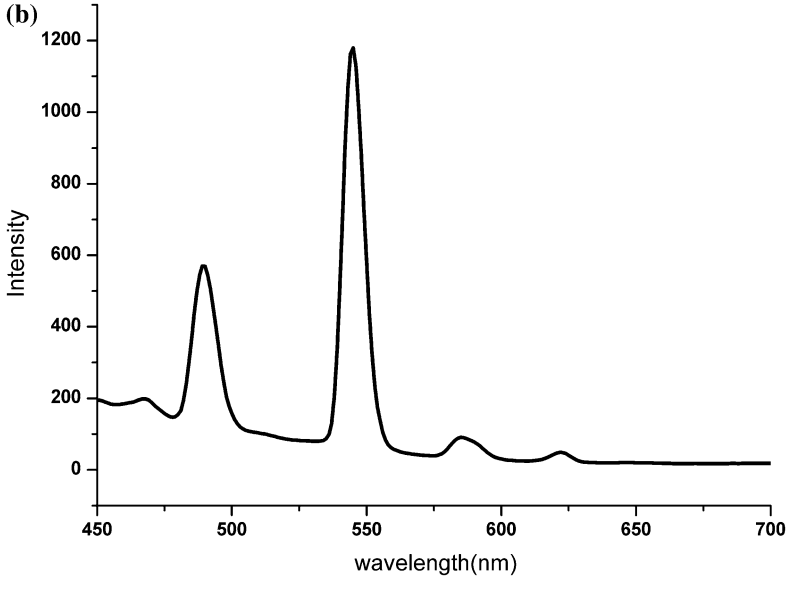

Figure 10b. Solid-state emission spectra at room temperature for **3**.

respectively. The Ln(III)–$O_{carbonyl}$ bond lengths decrease along the series from Eu to Tm for both Ln(1) and Ln(2) centers, as also reported by Liu's group [9]. The effect of lanthanide contraction can also be observed through changes in the organic linker. Because

Table 2. Selected bond lengths (Å) for **1–8**.

1	Eu1–O1	2.6166(37)	**2**	Gd1–O1	2.4042(62)	**3**	Tb1–O1	2.3886(62)
	Eu1–O2	2.4208(42)		Gd1–O2	2.6091(43)		Tb1–O2	2.6069(62)
	Eu1–O4	2.3291(29)		Gd1–O4	2.3153(38)		Tb1–O4	2.3033(39)
	Eu1–O6	2.3736(33)		Gd1–O6	2.3047(38)		Tb1–O6	2.2853(40)
	Eu1–O8	2.3878(27)		Gd1–O8	2.3765(36)		Tb1–O8	2.3325(44)
	Eu1–O10	2.3234(32)		Gd1–O10	2.3537(36)		Tb1–O10	2.3611(37)
	Eu2–O3	2.4773(32)		Gd2–O3	2.4653(36)		Tb2–O3	2.4543(54)
	Eu2–O5	2.3995(27)		Gd2–O5	2.3970(35)		Tb2–O5	2.3821(38)
	Eu2–O7	2.3325(33)		Gd2–O7	2.3896(36)		Tb2–O7	2.3768(43)
	Eu2–O9	2.3293(28)		Gd2–O9	2.3173(38)		Tb2–O9	2.3123(39)
	Eu2–O11	2.4100(26)		Gd2–O11	2.3192(38)		Tb2–O11	2.3085(54)
	Average	2.4000		Average	2.3865		Average	2.3737
4	Dy1–O1	2.3689(61)	**5**	Ho1–O1	2.2929(40)	**6**	Er1–O1	2.2916(34)
	Dy1–O2	2.6064(58)		Ho1–O4	2.2285(48)		Er1–O4	2.3124(35)
	Dy1–O4	2.2795(39)		Ho1–O8	2.3169(38)		Er1–O8	2.3627(36)
	Dy1–O6	2.2653(37)		Ho1–O6	2.2823(38)		Er1–O6	2.2134(39)
	Dy1–O8	2.3172(37)		Ho1–O10	2.3625(40)		Er1–O10	2.2736(36)
	Dy1–O10	2.3446(36)		Ho2–O2	2.3866(42)		Er2–O2	2.3860(36)
	Dy2–O3	2.4274(36)		Ho2–O3	2.5283(42)		Er2–O3	2.5316(35)
	Dy2–O5	2.3627(36)		Ho2–O5	2.3114(45)		Er2–O5	2.3349(36)
	Dy2–O7	2.3569(36)		Ho2–O9	2.3554(39)		Er2–O9	2.2595(37)
	Dy2–O9	2.2893(37)		Ho2–O7	2.2665(40)		Er2–O7	2.2978(37)
	Dy2–O11	2.2825(39)		Ho2–O11	2.2813(43)		Er2–O11	2.2588(36)
	Average	2.3546		Average	2.3284		Average	2.3202
7	Tm1–O1	2.2865(39)	**8**	Y1–O1	2.2993(31)	**9**	Lu1–O1	2.3393(56)
	Tm1–O4	2.2610(39)		Y1–O4	2.2174(35)		Lu1–O2	2.4173(45)
	Tm1–O8	2.3488(40)		Y1–O8	2.3150(29)		Lu1–O3	2.3911(67)
	Tm1–O6	2.2988(39)		Y1–O6	2.2742(28)		Lu1–O4	2.3226(55)
	Tm1–O10	2.2004(42)		Y1–O10	2.3726(33)		Lu1–O5	2.2260(48)
	Tm2–O2	2.5204(38)		Y2–O2	2.3873(33)		Lu1–O6	2.2265(48)
	Tm2–O3	2.3741(42)		Y2–O3	2.5304(30)		Lu2–O7	2.2411(45)
	Tm2–O5	2.2398(42)		Y2–O5	2.3080(35)		Lu2–O8	2.2327(47)
	Tm2–O9	2.2977(46)		Y2–O9	2.3424(37)		Lu2–O9a	259,348
	Tm2–O7	2.3256(38)		Y2–O7	2.2585(34)		Lu2–O11	2.2266(53)
	Tm2–O11	2.2507(41)		Y2–O11	2.2649(31)		Lu2–O12	2.2601(49)
	Average	2.3094		Average	2.3876		Lu2–O10	2.2445(57)

Table 3. Angles of coordinated SDB for **1–7**.

	1(Eu)	**2**(Gd)	**3**(Tb)	**4**(Dy)	**5**(Ho)
C1–S1–C2	101.665	101.262	101.105	100.711	105.178
C3–S2–C4	99.207	98.899	98.591	99.161	95.475
C5–S3–C6	100.079	99.585	99.392	98.451	96.155
C7–S4–C8	99.207	98.899	98.591	99.161	95.475
C9–S4–C10	100.079	99.585	99.392	98.451	96.155
Angle average	100.047	99.646	99.414	99.187	97.689
	6(Er)	**7**(Tm)			
C1–S1–C2	105.274	104.968			
C3–S2–C4	95.395	95.433			
C5–S3–C6	96.076	95.965			
C7–S4–C8	95.395	95.433			
C9–S4–C10	96.076	95.965			
Angle average	97.643	97.553			

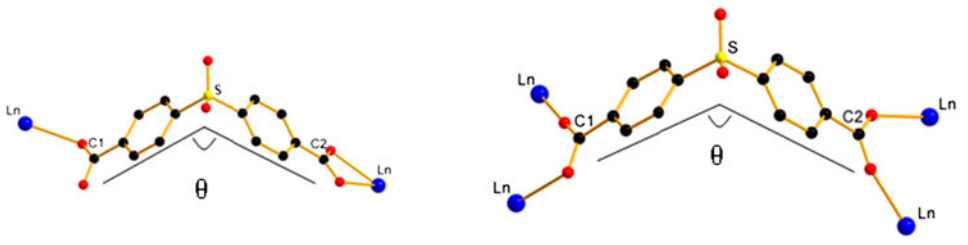

Figure 11. The angles of coordinated SDB.

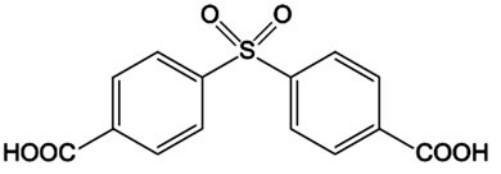

Chart 1. The H_2SDB ligand.

H_2SDB is a semirigid linker, the C–S–C angle can be altered during the synthesis of the MOFs. As shown in table 3, the C_1–S–C_2 (figure 11) bond angles for the six-coordinate SDB ligands decrease across the series from Eu to Tm. It is possible that the reason for this trend is that as the radii of the lanthanide(III) ions decrease, the strain on each coordinated SDB ligand by the Ln(III) ions located on either end of the ligands is reduced. Because of the lanthanide contraction effect, the chemical properties of Y(III) is similar to those of Ho(III), Er(III) and Tm(III), which explains why the crystal structure of Y-MOFs is very similar to those. This is proven by the isostructural MOFs – **5**, **6**, **7** and **8** described here (chart 1).

Conclusion

Nine coordination polymers of Ln(III)-SDB have been synthesized under hydrothermal conditions. A series of isostructural 2-D weaving structures are obtained with Ln(III) [Eu(**1**), Gd(**2**), Tb(**3**), Dy(**4**)]. Similar interspersed structures are also obtained by the one-pot reaction of Ln(III) [Ho(**5**), Er(**6**), Tm(**7**), Y(**8**)] and H_2SDB, but the same synthesis using Lu(III) results in a 1-D chain structure. As a semirigid V-shaped ligand, H_2SDB generates the paddlewheel structures with the metal ions for the design of coordination compounds containing H_2SDB. Lanthanide contraction in this series leads to decreases in the average Ln–O bond lengths and the average C–S–C bond angles of H_2SDB from **1–7**. TGA show that **1–7** exhibit high thermal stability. Furthermore, **1** and **3** exhibit interesting luminescent behavior, indicating that these complexes may be suitable candidates for optical materials.

Electronic supplementary information (ESI) available

CCDC 1014888-1014896 contain the supplementary crystallographic data for **1–9**. PXRD patterns, table of selected bond distances and angles for **1–9**, the FTIR spectra figures for **1–9**.

Disclosure statement

No potential conflict of interest was reported by the authors.

Funding

This work was financially supported by the National Nature Science Foundation of China [grant number 20971047], [grant number 21271076], [grant number 21471060]; Key Program of Guangdong Universities Science and Technology innovation [grant number cxzd1020]; Planning Program of Guangzhou City Science and Technology [grant number 2013J4100049].

References

[1] (a) M.D. Allendorf, C.A. Bauer, R.K. Bhakta, R.J.T. Houk. *Chem. Soc. Rev.*, **38**, 1330 (2009); (b) Y.J. Cui, Y.F. Yue, G.D. Qian, B.L. Chen. *Chem. Rev.*, **112**, 1126 (2012); (c) H.L. Jiang, Q. Xu. *Chem. Commun.*, **47**, 3351 (2011).

[2] (a) Y.F. Zhou, F.L. Jiang, D.Q. Yuan, B.L. Wu, R.H. Wang, Z.Z. Lin, M.C. Hong. *Angew. Chem. Int. Ed.*, **43**, 5665 (2004); (b) B. Zhao, P. Cheng, X.Y. Chen, C. Cheng, W. Shi, D.Z. Liao, S.P. Yan, Z.H. Jiang. *J. Am. Chem. Soc.*, **126**, 3012 (2004); (c) L. Pan, K.M. Adams, H.E. Hernandez, X. Wang, C. Zheng, Y. Hattori, K. Kaneko. *J. Am. Chem. Soc.*, **125**, 3062 (2003).

[3] (a) M. O'Keeffe. *Chem. Soc. Rev.*, **38**, 1215 (2009); (b) O.M. Yaghi, Q. Li. *MRS Bull.*, **34**, 682 (2009).

[4] (a) N. Kerbellec, L. Catala, C. Daiguebonne, A. Gloter, O. Stephan, J.-C. Bünzli, O. Guillou, T. Mallah. *New J. Chem.*, **32**, 584 (2008); (b) K. Liu, H. You, Y. Zheng, G. Jia, Y. Song, Y. Huang, M. Yang, J. Jia, N. Guo, H. Zhang. *J. Mater. Chem.*, **20**, 3272 (2010); (c) J.-M. Herrera, S.J.A. Pope, H. Adams, S. Faulkner, M.D. Ward. *Inorg. Chem.*, **45**, 3895 (2006).

[5] (a) Z. Wang, Y.H. Xing, C.G. Wang, L.X. Sun, J. Zhang, M.F. Ge, S.Y. Niu. *CrystEngComm*, **12**, 762 (2010); (b) R. Chakrabarty, P.S. Mukherjee, P.J. Stang. *Chem. Rev.*, **111**, 6810 (2011); (c) K. Davies, S.A. Bourne, C.L. Oliver. *Cryst. Growth Des.*, **12**, 1999 (2012); (d) P. Thuery, B. Masci. *CrystEngComm*, **12**, 2982 (2010); (e) J. Zhao, L.S. Long, R.B. Huang, L.S. Zheng. *Dalton Trans.*, **35**, 4714 (2008).

[6] Y.H. Luo, F.X. Yue, X.Y. Yu, X. Chen, H. Zhang. *CrystEngComm*, **15**, 6340 (2013).

[7] (a) D.S. Raja, J.H. Luo, C.Y. Wu, Y.J. Cheng, C.T. Yeh, Y.T. Chen, S.H. Lo, Y.-L. Lin. *Cryst. Growth Des.*, **13**, 3785 (2013); (b) Y.Q. Sun, J. Zhang, Y.M. Chen, G.Y. Yang. *Angew. Chem. Int. Ed.*, **44**, 5814 (2005).

[8] W.T. Xu, Y.F. Zhou, D.C. Huang, W. Xiong, M.Y. Su, K. Wang, S. Han, M.C. Hong. *Cryst. Growth Des.*, **13**, 5420 (2013).

[9] J.X. Liu, Y.F. Hu, R.L. Lin, W.Q. Sun, X.F. Chu, S.F. Xue, Q.J. Zhu, Z. Tao. *CrystEngComm*, **14**, 6983 (2012).

[10] (a) X.L. Wang, C. Qin, E.B. Wang, Y.G. Li, Z.M. Su, L. Xu, L. Carlucci. *Angew. Chem. Int. Ed.*, **44**, 5824 (2005); (b) X.L. Wang, C. Qin, E.B. Wang, Z.M. Su. *Chem. Eur. J.*, **12**, 2680 (2006); (c) J. Tao, J.X. Shi, M.L. Tong, X.X. Zhang, X.M. Chen. *Inorg. Chem.*, **40**, 6328 (2001); (d) D.F. Sun, R. Cao, Y.Q. Sun, W.H. Bi, X.J. Li, Y.Q. Wang, Q. Shi, X. Li. *Inorg. Chem.*, **42**, 7512 (2003).

[11] (a) Y. Hijikata, S. Horike, M. Sugimoto, M. Inukai, T. Fukushima, S. Kitagawa. *Inorg. Chem.*, **52**, 3634 (2013); (b) S. Bhattacharya, K.V. Ramanujachary, S.E. Lofland, T. Magdaleno, S. Natarajan. *CrystEngComm*, **14**, 4323 (2012); (c) W.J. Zhuang, H.L. Sun, H.B. Xu, Z.M. Wang, S. Gao, L.P. Jin. *Chem. Commun.*, **46**, 4339 (2010).

[12] W.J. Zhuang, X.J. Zheng, H.L. Sun, L.P. Jin. *Chin. J. Inorg. Chem.*, **24**, 1305 (2008).

[13] (a) G.M. Sheldrick, *SHELXL97*, Göttingen (1997); (b) D. Santamaria-Perez, A. Vegas, C. Mühle, M. Jansen. *Acta Cryst. B*, **67**, 109 (2011); (c) Bruker. *APEX II, SAINT*, Bruker AXS Inc., Madison, WI (2004).

[14] (a) W. Ouellette, B.S. Hudson. *J. Zubieta. Inorg. Chem.*, **46**, 4887 (2007); (b) C.M. Che, H.Y. Chao, V.M. Miskowski, Y.Q. Li, K.K. Cheung. *J. Am. Chem. Soc.*, **123**, 4985 (2001); (c) X. He, C.Z. Lu, D.Q. Yuan. *Inorg. Chem.*, **45**, 5760 (2006); (d) Q. Wu, M. Esteghamatian, N.X. Hu, Z. Popovic, G. Enright, Y. Tao, M.

D'Iorio, S. Wang. *Chem. Mater.*, **12**, 79 (2000); (e) J.E. McGarrah, Y.J. Kim, M. Hissler, R. Eisenberg. *Inorg. Chem.*, **40**, 4510 (2001).
[15] J.L. Song, J.G. Mao. *Chem. Eur. J.*, **11**, 1417 (2005).
[16] G.L. Law, K.L. Wong, X. Zhou, W.T. Wong, P.A. Tanner. *Inorg. Chem.*, **44**, 4142 (2005).
[17] H.M. Peng, H.G. Jin, Z.G. Gu, X.J. Hong, M.F. Wang, H.Y. Jia, S.H. Xu, Y.P. Cai. *Eur. J. Inorg. Chem.*, **33**, 5562 (2012).